

RELEVANCE AND LOCI OF ODORANT FEATURES IN THE RAT OLFACTORY BULB

Statistical Methods for Understanding Olfactory Codes in Glomerular Images

Benjamin Auffarth, Agustín Gutierrez–Galvez and Santiago Marco

Intelligent Signal Processing group, Department of Electronics, University of Barcelona

Artificial Olfaction group, Institute for Bioengineering of Catalonia (IBEC), C/Baldri Reixac 13, 08028 Barcelona, Spain

Keywords: Olfactory coding, Olfactory bulb, Odorants, Glomeruli, Property–activity relationship, Classification, Non-parametric statistics.

Abstract: The relationship between physicochemical properties of odor molecules and perceived odor quality is arguably one of the most important issues in olfaction and the rules governing this relationship remain unknown. Any given odor molecule will stimulate more than one type of receptor in the nose, perhaps hundreds, and this stimulation reflects itself in the neural code of the olfactory nervous system. We present a method to investigate neural coding at the glomerular level of the olfactory bulb, the first relay for olfactory processing in the brain. Our results give insights into localization of coding sites, relevance of odorant properties for information processing, and the size of coding zones.

1 INTRODUCTION

Animals are able to recognize a large number of different odors (Axel, 1995) and this is crucial in social interaction, feeding, and mating. This discriminatory performance is due to a series of information processing steps at several levels of the olfactory system, beginning from graded affinity of olfactory receptors to different odors. Depending on the animal, there are several hundred olfactory receptor types, in particular about 1000 types in the rat (Buck and Axel, 1991), the transaction principles of which is presently not well understood. Apparently, there are no molecular features of the odorant that directly determine perceptive quality (Sell, 2006).

It has been experimentally found (Malnic et al., 1999) that each receptor type responds to a broad range of odorants and each odorant evokes responses from many different receptor types. The odotope theory (Mori and Shepherd, 1994) is the prevalent view on olfactory transduction and proposes that each olfactory receptor detects a combination of structural molecular features, although it is not clear which these features are. These combinations of features are called odotopes in analogy with epitopes, the antigenic determinant of the immune system. Each odorant molecule contains many different properties and

the information about the odorant would then be encoded by the combined responses of many types of receptors, each of which recognizes a specific subset.

Axons from olfactory neurons are bundled in neuropil structures in the olfactory bulb, called glomeruli, in a way that each glomerulus receives axons just from one type of receptor (Bozza et al., 2002). It is well-established that there is a systematic spatial coding of chemical properties in glomerular activations (Johnson et al., 1998; Johnson and Leon, 2007) in the way that odorants with different chemical structure and shape generate distinct patterns of glomerular activation. It has also been found that in the rat olfactory bulb certain properties correlate with activation in certain zones (Uchida et al., 2000; Johnson and Leon, 2000; Mori et al., 2006; Johnson et al., 2007).

In this paper, we present a method to analyze several aspects of property–activation relationships in rat glomerular coding of odorants. The questions we investigate are: which odorant properties are coded and where, what is the size of the coding zones, and how relevant are individual odorant properties to the encoding. The last question should also give us information about relevance of odorant properties to olfactory processing and thereby their contribution to perception of odor quality.

Our techniques consisted of a nonparametric sta-

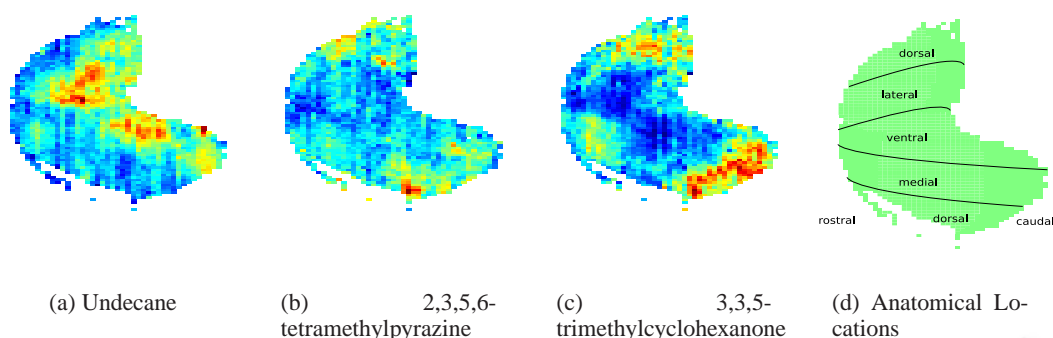


Figure 1: Glomerular activity in response to three odorants and anatomical locations in the olfactory bulb. In the response maps, red stands for high activation, blue for low activation. It can be seen that odorants can be distinguished – to some extent – by the spatial activation of glomeruli. 1(a) shows responses to the odorant undecane, which is an alkane (compare 2(a)). Pixel intensities in 1(b) express activation in response to 2,3,5,6-tetramethylpyrazine, which is an aromatic (compare figure 2(c)). In 1(c) responses to 3,3,5-trimethylcyclohexanone (CAS number 873-94-9) can be seen. This last odorant is a ketone (compare 2(e)). The rightmost subfigure, 1(d), denominates locations in anatomical terms for the glomerular layer of the rat olfactory bulb. This was adapted from (Johnson et al., 1999).

tistical test with bootstrapping, and support–vector machine classification. Information of these techniques should reveal relevance of odorant properties, and localization and size of coding zones.

We will explain first the data set, then in the methods section we explain how we approached the questions, before we look at results, discuss them, and draw conclusions.

2 DATA SET

In this study we used a set of images of glomerular responses in the rat olfactory bulb (Johnson et al., 2006) provided by the group around Michael Leon and Brett Johnson at the University of California, Irvine. The images were taken by 2–deoxyglucose autoradiography and covered the entire lamina. They took measurements at systematic angle increments around equally spaced coronal bulb sections. Their technique has the advantages to work with unanesthetized, freely respiring animals and gives the ability to analyze the entire glomerular layer. On the other hand, it does not record temporal dynamics of the olfactory response and it is impossible to compare responses in the same animal.

Each of these images corresponds to glomerular responses to one particular odorant. Examples from this data set can be seen in figure 1, which shows glomerular responses to two odorants.

We mean–centered all pixels to have maps that show activation at each pixel relative to its overall pattern, and normalized deviations to standard unit to compensate for differences in absolute pixel intensi-

ties. We started with 472 maps, some of which representing responses to identical odorants in different concentrations. We took means over concentrations and discarded a few activity maps for which we did not have the information of the odorant. This pre–processing left us with 308 maps corresponding to distinct and known odorants.

There were missing values in some images. In the bottom–left of ventral–centered charts they were caused by loss of tissue on the knife during cryosectioning. Missing values in the central–right parts of the image were principally due to loss of tissue during removal of the bulbs from the skull using microdissecting scissors. Pixels that had missing values in any of the images were ignored in the analysis, which left us with 1834 pixels.

After pre–processing, the data set was a matrix $M \in \mathbb{R}^{308,1834}$ of activations. Each of the 1834 *pixels* of this matrix, $p \in \mathbb{R}^{308}$, represented responses of the same glomerulus to different odorants.

For all activation maps that remain after pre–processing we had the information concerning which odorant they correspond to and additional descriptive information also provided by the Leon Lab. Descriptors, about 200 in total, included physicochemical odorant properties as well as perceptual properties ascribed to the sensed odor. Properties were of continuous and binary type. Continuous properties include molecular length, height, and weight. To give some examples of binary properties, binary properties concerned cyclization (whether an odorant is alicyclic, aromatic, polycyclic, or heterocyclic), bond saturation (whether an odorant is alkene, alkane, or alkyne), and functional groups (whether an odorant is

ester or lactone, amine, carboxylic acid, contains sulfur, contains halogen, is a ketone, alcohol or phenol). Perceptual properties are all binary and included flavors such as sweet, camphoraceous, floral, and minty. For some properties there were many associated activity maps, for some very few. We had to discard many because of insufficient representation in the data.

3 METHODS

3.1 Localization of Coding Zones

One of our goals in this research is to determine the activation loci for each property. This is to say, finding the bulbar zones that encode for each property if such a zone exists.

For each point in the maps and each odorant or perceptual property, we tested statistically whether the given pixel shows significant differences with respect to the property. For binary properties we compared activations on images, where a property was given, with activations on images, where property was not given using a statistical test.

For some properties, we had only very few images that corresponded to them. To account for statistical variations in these distributions we used a bootstrap (Efron, 1982) procedure to estimate p -values of the statistical test.

The application of the bootstrap to test and derive confidence intervals and p -values was introduced by (Felsenstein, 1985). Statistical analysis is repeatedly applied to subpopulations of the same size, generated by sampling from the original population with replacement. Bootstrap methods can be used for hypothesis tests, calculating confidence intervals and regression analysis.

The Wilcoxon ranked-sum test (also called Mann-Whitney U test) assesses whether two samples come from the same distribution (null hypothesis). It is analogous to applying the student t -test on the data after ranking over the combined samples. It has the advantage of not assuming normality and of more robustness with respect to the t -test and allows the two samples to be of arbitrary (unequal) size. The assumptions of the Wilcoxon rank-sum test are independence of the two samples and independence of observations within samples, and that the data are comparable. These assumptions are true for our data set. Our two samples are the activations given the binary property and the activations not given the binary property. The two samples are independent from each other and activations within samples are also indepen-

dent. They represent the same space, that of activations, hence they are comparable.

At each iteration we randomly sampled from the two distributions with replacement before applying the Wilcoxon rank-sum test. The resulting distribution of p -values was log-normal and we took the medians of p -values as bootstrap statistics and used these median p -values for subsequent analysis (Limpert et al., 2001). As estimation of the bootstrap error, we took the interquartile range of the sampled p -values. We found that there was a very high and very significant Pearson correlation between error and p -values ($\rho = 0.77$, $p = 0.001$). About 94% of points below significance level 0.05 had an associated error below 0.1. We only took these points into account (in order to exclude spurious results).

This method avoids the need to make assumptions about the shape of the distribution, such as normality, and uses instead the observed distributions of our data.

We say that points are coding for a (binary) property if the null hypothesis could be rejected at the 5% significance level.

For continuous properties the procedure was more involved. We discretized properties by grouping their values into bins, taking bin numbers as first guess from Sturges' formula (cf. (Wand, 1997)) then adjusting so that in each bin there were at least roughly 5% of activation maps. We then applied the procedure with bootstrap and Wilcoxon rank-sum test for differences between activations in response to property values in a particular bin versus activations in response to values out of bin, i. e. testing whether points corresponded to different ranges of the distribution of the chemical property.

3.1.1 Size of Coding Zones

We investigated the sizes of the zones that coded for properties. In order to determine the size of coding zones for a property, we defined the size as the number of points that were found to be significantly different with respect to the property.

Skewed distributions for some properties could have an impact on how many points are found to be significantly related to a property. By the statistical test it should be much more difficult for very skewed distributions to pass the significance threshold. In this paper, for size of coding zones, we take only into account 13 binary molecular properties, where at least 4 images were available. It is important to note that for these properties, data availability (odorants corresponding to presented odorant properties) and size of coding zone show no significant Pearson correlation ($\rho = 0.33$, $p = 0.27$).

3.2 Classification

The method presented in this subsection is based on the idea that classification performance between glomerular activation and odorant features can give information about this structure–activation relationship. Specifically we take the classification performance to compare relevances of properties to glomerular coding. We performed classification using a linear support vector machine (SVM) from glomerular activations as input vector and each property (present vs. not present) as target. In each of 10 iterations we randomly sampled half of the activation maps as training set and took the other half as test.

We distinguished between two experimental conditions:

1. best points – classification using most representative points, and
2. random baseline – classification using randomly sampled points.

For the first experimental condition, for each property, we ranked points by their significance with respect to the property (p -values from Wilcoxon rank–sum test) and then classified taking the best n points, with $n \in N = [1, 5, 10, 15, 20, 25, 30, 45, 50, 60, 70, 80, 90, 100, 110, 120, 130, 140, 150, 200, 300, 400, 500, 600, 700, 800, 900, 1000, 1100, 1200, 1300, 1400, 1500, 1600, 1700, 1834]$. As a random baseline, for each property, we took the same intervals from N , but randomly sampled points. We averaged over 250 random subsamples of points for each interval.

The scarceness of data for some properties brought about problems. We found that two commonly used SVM implementations, SvmLight and libsvm, are lacking robustness to tackle our problem. Because of this we used an in–house SVM classifier implemented in Matlab. We used the area under the ROC curve (AUC) as performance criterion. It has the advantage to be unbiased by skewed class distributions, which are a particular problem in our data set. An example of such an experimental run for the aromatic property is shown in figure 3.

4 RESULTS

4.1 Localization of Coding Zones

Figure 2 shows loci of coding zones for the 13 molecular properties.

In figure 2(a), colors indicate where significant differences with respect to alkane were found. This

subfigure is to illustrate results from the statistical determination of coding zones for a single property.

For the other chemical properties displayed in figure 2 we grouped properties into molecular bonds, cyclization, and functional groups. We created a factorial code so that the color code accounts for all combinations of coding for properties. For n properties, numbers from 0 to $n - 1$ were assigned to each property. For each point, a binary vector expresses whether a property was found to significant or not. The i th position in this vector stands for property i . Each vector represents a subset of all possible combinations $b_{prop} \in \{0, 1\}^n$. Each subset was assigned its distinct color.

Colors in figures in 2 show all combinations of properties that were encountered. To give an example, in 2(b) there are seven kinds of zones that mark codes for different combinations of properties alkane, alkene, and alkyne. Zones 1, 2, and 4 code for exclusively one of these properties. Zone 3 encodes alkane and alkene, zone 5 alkane and alkyne, zone 6 alkene and alkyne, and finally zone 7 codes for all of the three properties.

Cyclization properties, especially alicyclic, have a moderate but highly significant Pearson correlation ($\rho = 0.33$, $p = 2.05e - 9$ between alicyclic and polycyclic, $\rho = 0.36$, $p = 6.72e - 11$ between alicyclic and heterocyclic, and $\rho = 0.21$, $p = 1.95e - 04$ between aromatic and heterocyclic). As can be seen in 2(c) and 2(d), properties aromatic and heterocyclic and properties alicyclic and polycyclic, respectively, project to very similar bulbar regions. Functional groups did not have a high covariance, however there are many properties (6). To provide clearer figures, we split coding zones of both, cyclization and functional groups into two figures.

4.1.1 Size of Coding Zones

Table 1 shows size of coding zones as estimated. From the table it can be seen that aromatic is broadly coded by glomerular activations. Nearly 60% of points were found to show differences significant at the 5% level. Alkane covers the second biggest area with about 40% of points. Carboxylic acid and ketone are coded by about a third of all points. Coding zones for properties alkene, alicyclic, and heterocyclic extend to between about 20 and 30%. For ester+lactone, alkyne, and alcohol+phenol coding zones we measured between 10 and 16 percent of total. Properties polycyclic, sulfur–containing compound and amine recruit the smallest zones of compared properties with about 7%, 4%, and 0.6%, respectively.

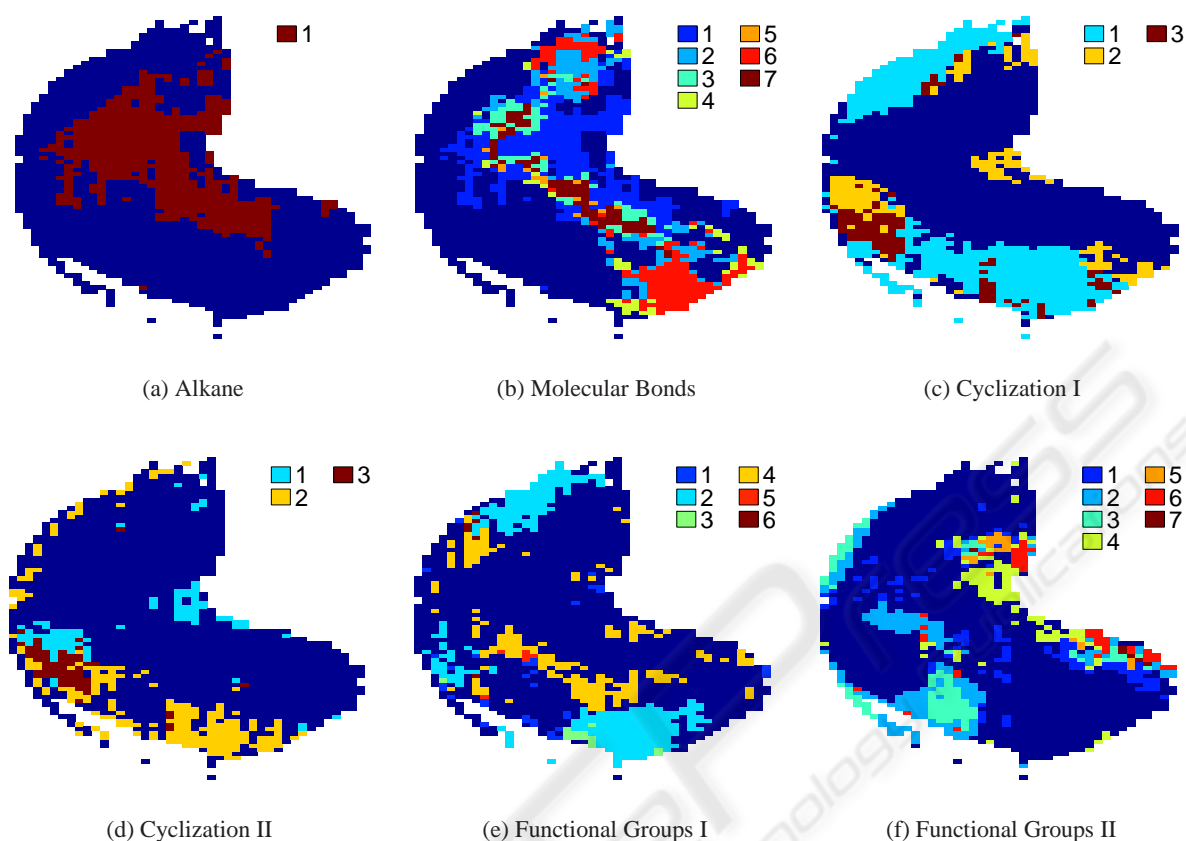


Figure 2: Localization of Molecular Properties: Maps with coding zones for various odorant properties. Loci of the 13 binary properties, grouped into basic dimensions molecular bonds, cyclization, and functional groups. Colors in figures serve to distinguish zones, which coded for a specific combination of several binary properties. For space efficiency legends refer to numbers which are explained in this caption. Factorial maps for all properties of cyclization and functional groups, respectively, were too crowded and therefore each were broken into two to be better intelligible. **2(a)** shows the coding zone for the alkane property as an demonstration of results of our statistical method of loci determination for a single property. **1** marks the coding zone for alkane. In **2(b)**, which represents molecular bond properties, the numbers stand for: **1** alkane **2** alkene **3** alkane, alkene **4** alkyne **5** alkane, alkyne **6** alkene, alkyne **7** alkane, alkene, alkyne. **2(c)** shows **2** cyclization properties. The number code is as follows: **1** polycyclic **2** heterocyclic **3** polycyclic and heterocyclic. **2(d)** shows the other **2** cyclization properties. The number code is as follows: **1** polycyclic **2** heterocyclic **3** polycyclic and heterocyclic. **2(e)** highlights coding zones for **3** functional group properties. The number code explained: **1** amine **2** ketone **3** amine and ketone **4** alcohol-phenol **5** amine and alcohol-phenol **6** ketone and alcohol-phenol. **2(f)** details loci for the other **3** functional group properties. The numbers: **1** ester+lactone **2** carboxylic acid **3** ester+lactone and carboxylic acid **4** sulfur-containing compound **5** ester+lactone and sulfur-containing compound **6** carboxylic acid and sulfur-containing compound **7** ester+lactone, carboxylic acid and sulfur-containing compound. Compare with table 1 where estimations of coding zone size are listed.

4.2 Classification

Here we present only results pertaining to 13 molecular properties, for which at least 4 images were available. It is important to note that Pearson correlation between classification performance and availability of data was low and very insignificant ($\rho = 0.2$, $p = 0.5$).

Table 2 ranks properties according to the classification performance (AUC) of the linear SVM. The classification performance is indicated in the second column.

Of the 13 compared properties, sulfur-containing compound, alkyne, alkane, alkene, and amine perform close to ceiling. Classifications of carboxylic acid, aromatic, and ketone also shows good performances. Polycyclic, ester-lactone, the functional group alcohol+phenol, and cyclization properties heterocyclic and alicyclic gives mediocre performances.

Table 1: Sizes of Coding Zones. The table shows for each property the numbers of points found to be significantly correlated at 5% significance level.

property	size of zone
aromatic	1070
alkane	717
carboxylic acid	646
ketone	459
alkene	424
alicyclic	399
heterocyclic	315
ester+lactone	296
alkyne	254
alcohol+phenol	204
polycyclic	125
sulfur-containing compound	76
amine	10

Table 2: Classification performance of odorant properties. The second column shows the maximum classification performance (in AUC) that was achieved in baseline or representative conditions (whichever was best).

property	max performance
sulfur-containing compound	0.99
alkyne	0.99
alkane	0.99
alkene	0.99
amine	0.99
carboxylic acid	0.93
aromatic	0.86
ketone	0.78
polycyclic	0.76
ester+lactone	0.75
alcohol+phenol	0.73
heterocyclic	0.73
alicyclic	0.72

5 DISCUSSION

5.1 Localization and Size of Coding Zone

We confirmed that for certain properties coding sites are clustered in zones. This could be the result of an optimization for local processing of feature combinations (Laughlin and Sejnowski, 2003). Figure 2 illustrates some of the properties pertaining to important coding dimensions as proposed by Johnson and Leon (Johnson and Leon, 2007). So far, our results of localization of properties seem to be in accordance with

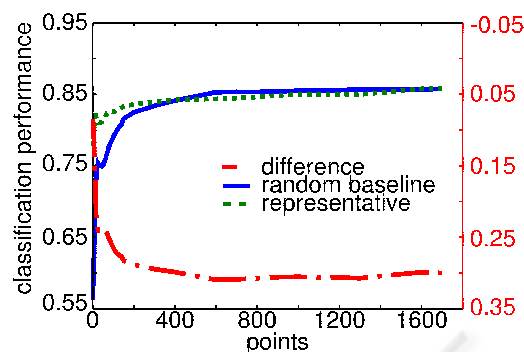


Figure 3: Classification Performance for Aromatic Property. The ordinate stands for the number of sampled points for classification. Curves depict performance in AUC with taking most representative points (solid line), randomly sampled points (dashed line), and the difference between the two (dash-dotted line).

literature.

As for the size of coding zone, it should be cautioned that results should be interpreted more qualitatively than quantitatively. The thresholding of p -values at certain significance values (here 5%) brings with it that effects of concentration and relevance cannot be completely separated from the size, however presented results can serve to group properties roughly by their coding zones.

There seem to be very few results in the literature on sizes of coding zones. Our results present a first step into the direction of quantifying different aspects of coding at the glomerular level. It seems there are huge differences with respect of size of coding zone. There are properties which recruit bigger zones and properties that recruit smaller zones. This could indicate that some properties are more specific with respect to the bulbar zone. Some more implications are discussed below together with the classification results.

5.2 Classification

We take classification performance of a molecular property to be indicative of its impact on early olfactory coding and — by implication — on perception. The logic behind is that properties that greatly change activations at the olfactory bulb level are easier to classify. Knowing the relevance of molecular properties could provide insight into early coding of chemical information and provide vital clues for discerning which properties are functional in determining the degree of interaction between an odorant receptor and odorant molecules.

For some properties, the performance curve from

representative points is below baseline at some intervals (compare figure 3). We think this to be because of the imperfect definition of most representative points. We define relevance as the best classification performance from either most representative points or random baseline whichever was higher.

The performance of the classification of amine found an early peak at 200 points, stayed at high levels until 600 points before leveling off drastically. The early peak could be explained by a very small area corresponding to amine (compare table 1) and in fact activation maps for amine looked very different from each other. Taking more points would not provide more information, rather noise, to the classification. We also think that the support vector machine had difficulties because of only very few data samples corresponding to amine (4 of 308 maps).

Activations are very distinct with respect to whether an odorant contained an sulfur-containing functional group or not. Bond saturation indicative of the reactionarity of compounds seems also to affect coding very strongly, as we can see in the high performance of alkyne, alkane, and alkene. Carboxylic acid another functional group and aromatic, a cyclization property, still seemed to be quite important. So far, our results confirm that cyclization, bond saturation, and some functional groups are very important. This is in line with Johnson and Leon (Johnson and Leon, 2007), who proposed as important dimensions of molecular properties cyclization, carbon numbers, bond saturation, branching, functional groups, and substitution position.

Our results can also be seen to partly confirm Yoshida and Mori (Yoshida and Mori, 2007) who proposed 14 primary odorant categories which could serve to enhance category-profile selectivity. These properties were sulfides, alcohols, methoxypyrazines, 6-carbon and 9-carbon green-odor compounds, aldehydes, ketones, isothiocyanates, terpene hydrocarbons, esters, terpene alcohols, alkylamines, acids, lactones, and phenol and its derivatives. We found that as for the properties included in this study, sulfides, alcohols-phenol, ketones, ester-lactone, amines, performance was quite good, however our results indicate that other properties such as whether odorants contained a carboxylic-acid group or their bond saturation could also be very important.

6 CONCLUSIONS

The glomerular level of the olfactory bulb is the first relay for olfactory processing in the brain. The information from the glomerular level is factored in sec-

ondary structures with cortical downstream to give the perception of odor. It has been confirmed that glomerular activations determine to some degree perceptual qualities of odorants (Cleland et al., 2002). There has been lot of investigation about which properties have most impact on perception or representation in the olfactory bulb, but we are not aware of any large-scale study to compare many different properties across a large data set. Our study is a first step into this direction.

We present a method to investigate coding at the glomerular level of the olfactory bulb and present results. Our method consisted of the application of the Wilcoxon rank-sum test within a bootstrap wrapper and the application of a support vector machine classification procedure.

By our statistical procedure we found coding zones in clustered glomeruli for several properties and the exact locations of coding zones. By extension we estimated the size of coding zones and found that investigated properties differed largely. The properties for which we found the smallest coding zones are amine and sulfur-containing compound, with roughly 0.5% and 4.1% of recruited area.

We then classified molecular properties by activation of glomerular activations in order to estimate relevance of properties. Our classification results indicate that there are some properties that affect odor coding on the olfactory bulb level very strongly. Most relevant properties we found to be alkyne, alkane, alkene, and amine. From our study, it could be derived the prediction that these properties have a very strong impact on perception (at least in rats).

Larger coding zones could mean that properties are broadly sensed by a range of olfactory receptors. In turn, it can be conjectured that properties which have a small coding zone in the olfactory bulb might have a more direct correspondence to olfactory receptor tuning. It could be hypothesized that properties with small coding zones could be more directly related to the proposed odotopes, especially so, properties that have high relevance to coding. There are other factors that influence size of coding zones, such as lateral connections between glomeruli that complicate matters, however – putting lateral connections aside – from the results in tables 1 and 2, amine, sulfur-containing compound, and alkyne could be candidates for odotopes.

ACKNOWLEDGEMENTS

The authors thank Miquel Tarzan for implementing a support vector machine that was robust enough to

make the classification study possible. One of the authors, B.A., is supported by a grant from the federal state government of Catalonia (formació de personal investigador, FI).

REFERENCES

- Axel, R. (1995). The molecular logic of smell. *Sci Am*, 273(4):154–9.
- Bozza, T., Feinstein, P., Zheng, C., and Mombaerts, P. (2002). Odorant Receptor Expression Defines Functional Units in the Mouse Olfactory System. *Journal of Neuroscience*, 22(8):3033–43.
- Buck, L. and Axel, R. (1991). A novel multigene family may encode odorant receptors: a molecular basis for odor recognition. *Cell*, 65(1):175–187.
- Cleland, T., Morse, A., Yue, E., and Linster, C. (2002). Behavioral models of odor similarity. *Behavioral neuroscience*, 116(2):222–231.
- Efron, B. (1982). The Jackknife, the Bootstrap and other re-sampling plans. In *CBMS-NSF Regional Conference Series in Applied Mathematics, Philadelphia: Society for Industrial and Applied Mathematics (SIAM), 1982*.
- Felsenstein, J. (1985). Confidence limits on phylogenies: an approach using the bootstrap. *Evolution*, pages 783–791.
- Johnson, B., Xu, Z., Pancoast, P., Kwok, J., Ong, J., and Leon, M. (2006). Differential specificity in the glomerular response profiles for alicyclic, bicyclic and heterocyclic odorants. *The Journal of comparative neurology*, 499(1):1–16.
- Johnson, B. A., Arguello, S., and Leon, M. (2007). Odorants with multiple oxygen-containing functional groups and other odorants with high water solubility preferentially activate posterior olfactory bulb glomeruli. *Journal of Comparative Neurology*, 502(3):468–482.
- Johnson, B. A. and Leon, M. (2000). Odorant molecular length: One aspect of the olfactory code. *Journal of Comparative Neurology*, 426(2):330–338.
- Johnson, B. A. and Leon, M. (2007). Chemotopic odorant coding in a mammalian olfactory system. *Journal of Comparative Neurology*, 503:1–34.
- Johnson, B. A., Woo, C. C., Hingco, E. E., Pham, K. L., and Leon, M. (1999). Multidimensional chemotopic responses to n-aliphatic acid odorants in the rat olfactory bulb. *Journal of Comparative Neurology*, 409(4):529–548.
- Johnson, B. A., Woo, C. C., and Leon, M. (1998). Spatial coding of odorant features in the glomerular layer of the rat olfactory bulb. *Journal of Comparative Neurology*, 393(4):457–471.
- Laughlin, S. and Sejnowski, T. (2003). Communication in neuronal networks. *Science*, 301(5641):1870–1874.
- Limpert, E., Stahel, W., and Abbt, M. (2001). Log-normal distributions across the sciences: keys and clues. *Bio-science*, 51(5):341–352.
- Malnic, B., Hirono, J., Sato, T., and Buck, L. (1999). combinatorial receptor codes for odors. *Cell*, 96(5):713–723.
- Mori, K. and Shepherd, G. (1994). Emerging principles of molecular signal processing by mitral/tufted cells in the olfactory bulb. *Semin Cell Biol*, 5(1):65–74.
- Mori, K., Takahashi, Y., Igarashi, K., and Yamaguchi, M. (2006). Maps of odorant molecular features in the mammalian olfactory bulb. *Physiological reviews*, 86(2):409–433.
- Sell, C. (2006). On the unpredictability of odor. *Angewandte Chemie International Edition*, 45(38):6254–6261.
- Uchida, N., Takahashi, Y., Tanifuji, M., and Mori, K. (2000). Odor maps in the mammalian olfactory bulb: domain organization and odorant structural features. *Nature Neuroscience*, 3:1035–1043.
- Wand, M. P. (1997). Data-based choice of histogram bin width. *The American Statistician*, 51(1):59–64.
- Yoshida, I. and Mori, K. (2007). Odorant Category Profile Selectivity of Olfactory Cortex Neurons. *Journal of Neuroscience*, 27(34):9105–9114.